

in T_c . On the other hand, as reported earlier^{14,15} some transition metals (e.g., Ti and Zr) containing magnetic-element impurities in nonmagnetic state seem to exhibit increase in T_c . This would suggest that the two-body effects dominate the one-body interaction over certain impurity-concentration regions in these systems.

Such two-body interactions have also been found to be important for other physical properties, e.g., resistance minimum in alloys¹⁶ and semiconductors¹⁷ con-

taining impurities, thermoelectric power,¹⁸ and anomalous density of states,¹⁹ etc.

Recently, Fowler *et al.*²⁰ have discovered a positive isotope effect in α -uranium which suggests a mechanism for superconductivity other than that involving lattice deformation. This mechanism would involve an interaction of the conduction electrons with the electron cores resulting in the polarization of d (or f) electron shells. The mechanism considered by us,⁶ in conjunction with the phonon-induced process, may describe such electronic polarization effects in pure systems as well.

¹⁴ J. A. Cape and R. R. Hake, Phys. Rev. **139**, A142 (1965).

¹⁵ B. T. Matthias, V. B. Compton, H. Suhl, and E. Cornzvit, Phys. Rev. **115**, 1597 (1959).

¹⁶ B. N. Ganguly, U. N. Upadhyaya, and K. P. Sinha, Proc. Phys. Soc. (London) **90**, 445 (1967).

¹⁷ K. S. V. L. Narasimhan and K. P. Sinha, Can. J. Phys. **45**, 3029 (1967).

¹⁸ U. N. Upadhyaya and K. P. Sinha (to be published).

¹⁹ B. N. Ganguly, Phys. Letters **25A**, 262 (1967).

²⁰ R. D. Fowler, J. D. G. Lindsay, R. W. White, H. H. Hill, and B. T. Matthias, Phys. Rev. Letters **19**, 892 (1967).

Millimeter-Wave Mixing with Josephson Junctions

C. C. GRIMES AND SIDNEY SHAPIRO*

Bell Telephone Laboratories, Murray Hill, New Jersey

(Received 3 November 1967)

Experiments are reported in which two millimeter-wave signals incident on point-contact Josephson junctions produced changes in the junction dc voltage versus current characteristic and an intermediate frequency output whose amplitude depended sensitively on both junction bias and applied power. Equations are derived, based on Josephson's phenomenological equations, for the Josephson current in a junction exposed to two applied rf signals. When the applied signals differ appreciably in frequency, additional constant-voltage steps in the V - I curve are predicted which are spaced at the difference frequency. These steps have been observed in experiments employing sources at 64 and 72 Gc/sec. Results of mixing experiments utilizing two sources nearly equal in frequency are reported at 23 and at 72 Gc/sec. In this case the two waves beat together and are equivalent in their effect to a single signal amplitude modulated at the difference frequency. Also explained on the same basis are experiments in which the third harmonic of a signal at 24 Gc/sec mixed with a signal at 72 Gc/sec. These results demonstrate the existence of the Josephson mixing mechanism as opposed to classical nonlinear mixing, and they show that it is operative at microwave and millimeter-wave frequencies over a wide range of power.

I. INTRODUCTION

A LARGE number of high-frequency effects have been demonstrated by Josephson junctions^{1,2} formed from superconducting point contacts.³ Radio-frequency⁴ and microwave^{4,5} generation; microwave

harmonic generation⁶; rf,⁷ microwave,^{8,9} and far-infrared^{8,9} video detection have all been reported. In this paper we report the first extensive study of millimeter-wave mixing with point-contact Josephson junctions.

Two signals, either in the vicinity of 23 Gc/sec (13-mm wavelength) or in the vicinity of 72 Gc/sec (4-mm wavelength), were mixed in the Josephson junction. The mixing action was detected both by observing the difference-frequency signal directly and by observing modification of the dc voltage-current characteristic of the junction.

* Present address: Department of Electrical Engineering, University of Rochester, Rochester, N.Y. 14627.

¹ B. D. Josephson, Phys. Letters **1**, 251 (1962); Rev. Mod. Phys. **36**, 216 (1964); Advan. Phys. **14**, 419 (1965).

² P. W. Anderson, in *Lectures on the Many-Body Problem*, edited by E. R. Caianiello (Academic Press Inc., New York, 1964), p. 113; and in *Progress in Low Temperature Physics*, edited by C. J. Gorter (North-Holland Publishing Co., Amsterdam, 1967), Vol. V, p. 1.

³ J. E. Zimmerman and A. H. Silver, Phys. Rev. **141**, 367 (1966).

⁴ J. E. Zimmerman, J. A. Cowen, and A. H. Silver, Appl. Phys. Letters **9**, 353 (1966).

⁵ A. H. Dayem and C. C. Grimes, Appl. Phys. Letters **9**, 47 (1966).

⁶ S. Shapiro, J. Appl. Phys. **38**, 1879 (1967).

⁷ A. H. Silver and J. E. Zimmerman, Appl. Phys. Letters **10**, 142 (1967).

⁸ C. C. Grimes, P. L. Richards, and S. Shapiro, Phys. Rev. Letters **17**, 431 (1966).

⁹ C. C. Grimes, P. L. Richards, and S. Shapiro (to be published).

Two additional experiments were carried out and are reported in this paper. In one, a 13-mm signal and a 4-mm signal were mixed directly in a Josephson junction; in the other, two signals at roughly 4 mm, but separated in frequency by about 8 Gc/sec, were mixed in a junction.

It is necessary to distinguish between ordinary, or classical mixing, which occurs via a nonlinear impedance at the input frequencies,^{10,11} and Josephson mixing, which occurs via the nonlinear nature of Josephson currents. The nonlinear Josephson currents, of course, give rise to a nonlinear impedance and so both mixing mechanisms are present in a Josephson junction and, in fact, both were observed in our experiments. However, the two mechanisms are distinguishable since they give rise to different behavior of the observed signals. Furthermore, the classical mechanism is usually far less sensitive than the Josephson mechanism and appears at input signal levels so strong as to quench or nearly quench all Josephson behavior.

The purpose of our paper is to point out the Josephson mixing mechanism, to give an analysis of the effect based on Josephson's phenomenological equations, and to present experimental results which bear out the predictions of the analysis. Where appropriate, the contrast with the prediction of classical mixing theory is pointed out.

Our concern here is solely with the physical mechanism of the observed mixing action; no attention is paid to such important applied questions as detection sensitivity, mixer conversion loss, system noise figure, or impedance transformation.¹²

In Sec. II, a general analysis based on Josephson's phenomenological equations is given for a Josephson junction exposed to two applied rf signals. Expressions derived for cases appropriate to our experiments are used later to interpret the experimental results. Section III contains a description of pertinent experimental details. The experimental results are presented and discussed in Sec. IV for the four types of mixing experiment performed. The paper concludes, in Sec. V, with a summary of results and conclusions.

II. ANALYSIS OF THE JOSEPHSON MIXING MECHANISM

Josephson¹ has shown that the phase difference φ between the superconducting pair wave functions on

¹⁰ R. V. Pound, *Microwave Mixers* (McGraw-Hill Book Co., New York, 1948).

¹¹ Mixing of the classical type has been observed in ordinary superconducting tunnel junctions by S. Shapiro and E. J. McNiff, Jr., see final report on Superconductive Effects in Thin Films, March, 1964, AD439221 (unpublished).

¹² W. H. Higa [in Proceedings of the Conference on Electron Devices, Montreal, 1967 (unpublished)] reported a conversion loss of ≈ 6 dB and a system noise figure of ≈ 7 dB for point-contact Josephson junction mixers at 13 Gc/sec with an i.f. of 2.2 Gc/sec. G. K. Gaulé, R. L. Ross, and R. Schwidtal [in Proceedings of the Conference on the Physics of Superconducting Devices, Charlottesville, Va., 1967 (unpublished)] reported mixing in a Josephson junction between two signals at about 10 Gc/sec. They observed modifications in the junction $V-I$ curve, and they detected a 200-Mc/sec difference frequency.

each side of the barrier in a Josephson junction determines the Josephson current j that may pass through unit area of the barrier. He has demonstrated that the constitutive relation between j and φ can be expressed for weak-coupled junctions in the form

$$j = j_0 \sin \varphi, \quad (1)$$

where j_0 is given explicitly by the microscopic theory^{1,13,14} but is here treated as a phenomenological parameter equal to the maximum zero-voltage current that can be driven through the junction.

In Eq. (1), φ is an implicit function of space and time. Josephson has shown that the dependence on space and time is related, respectively, to the presence of magnetic fields and electric fields, i.e., voltages. He has given a pair of phenomenological differential equations for the space and time variations of φ in the junction. Once φ is determined, j follows from Eq. (1). These equations are, in cgs units,

$$\nabla \varphi = (2ed/\hbar c) \mathbf{H} \times \hat{n} \quad (2)$$

and

$$\partial \varphi / \partial t = 2eV/\hbar, \quad (3)$$

where the vector magnetic field \mathbf{H} and the voltage across the barrier V may be functions of space and time. In Eqs. (2) and (3), e is the magnitude of the electronic charge, c is the velocity of light, \hbar is Planck's constant divided by 2π , \hat{n} is a unit vector normal to the barrier, and d is a length used to specify the effective thickness of magnetic field penetration near the barrier. For a plane-parallel junction, d is given by the sum of the barrier thickness and the penetration depths in the superconductors on either side. To form a complete phenomenological set of equations Maxwell's equations must be added to Eqs. (1)–(3), together with boundary and initial conditions appropriate to the problem.

Of dominant concern in our experiments was the time dependence of the Josephson currents. Therefore, we shall assume in subsequent calculation that no magnetic fields are applied to the junction and φ is spatially uniform across the junction. Qualitatively, it is easy to see that magnetic fields modify the Josephson current terms present in zero field, and this was readily observed in our experiments. The quantitative modifications are tedious to calculate and were not studied experimentally. Additional effects may also be introduced by the presence of magnetic fields, such as those associated with possible junction self-resonances,¹⁵ but no attempt was made to identify such terms in our experiments.

Let V_0 represent the dc voltage impressed across the junction. Then, when rf voltages of magnitude v_1 and v_2 , and angular frequencies ω_1 and ω_2 , respectively,

¹³ V. Ambegoakar and A. Baratoff, *Phys. Rev. Letters* **10**, 486 (1963); **11**, 104 (E) (1963).

¹⁴ N. R. Werthamer, *Phys. Rev.* **147**, 255 (1966).

¹⁵ D. N. Langenberg, D. J. Scalapino, and B. N. Taylor, *Proc. IEEE* **54**, 560 (1966).

are applied, the total voltage V becomes

$$V = V_0 + v_1 \cos(\omega_1 t + \theta_1) + v_2 \cos(\omega_2 t + \theta_2), \quad (4)$$

where the phase factors θ_1 and θ_2 are taken with respect to some arbitrary zero of time. We assume for the time being that the frequencies ω_1 and ω_2 differ appreciably. From Eqs. (1), (3), and (4) and with the definition

$$\omega_0 = 2eV_0/\hbar, \quad (5)$$

we obtain

$$\frac{j}{j_0} = \sin \left\{ \omega_0 t + \varphi_0 + \frac{2ev_1}{\hbar\omega_1} \sin(\omega_1 t + \theta_1) + \frac{2ev_2}{\hbar\omega_2} \sin(\omega_2 t + \theta_2) \right\}, \quad (6)$$

where the integration constant φ_0 is the initial phase difference across the barrier in the absence of applied voltages. By using standard trigonometric identities and the relations¹⁶

$$\cos(X \sin\theta) = \sum_{n=-\infty}^{\infty} J_n(X) \cos n\theta \quad (7)$$

and

$$\sin(X \sin\theta) = \sum_{n=-\infty}^{\infty} J_n(X) \sin n\theta, \quad (8)$$

where $J_n(X)$ is the Bessel function of order n , Eq. (6) can be put in the form

$$\frac{j}{j_0} = \sum_{k=-\infty}^{\infty} \sum_{l=-\infty}^{\infty} J_k \left(\frac{2ev_1}{\hbar\omega_1} \right) J_l \left(\frac{2ev_2}{\hbar\omega_2} \right) \times \sin \{ \omega_0 t + \varphi_0 + k(\omega_1 t + \theta_1) + l(\omega_2 t + \theta_2) \}. \quad (9)$$

Equation (9) is the general expression for the Josephson currents, at all frequencies and voltages, in the presence of two applied rf voltages. It predicts the appearance of current steps at constant voltage not only for $\omega_0 = k\omega_1$ and $\omega_0 = l\omega_2$, which are well known from experiments with a single applied rf signal,¹⁷ but also for $\omega_0 = k\omega_1 \pm m\Delta\omega$ and $\omega_0 = l\omega_2 \pm n\Delta\omega$, where $\Delta\omega = \omega_1 - \omega_2$ and k, l, m , and n are integers. These additional steps form series spaced by the difference frequency $\Delta\omega$ from each of the steps associated directly with the two input frequencies. The most direct evidence for the Josephson mixing mechanism is provided by the amplitudes of these additional steps.

From Eq. (9) it is possible to write specific expressions for the Josephson current flowing at any given frequency on any given constant-voltage step. With both the dc voltage and the frequency of interest specified, the argument of the sine function in Eq. (9) is fixed and so possible sets of values of the integers k and l are determined. The expressions that result for each case of interest can be put into convenient form when use is made of a number of standard trigonometric

expressions and the relation

$$a \cos x + b \sin x = (a^2 + b^2)^{1/2} \cos[x - \tan^{-1}(b/a)]. \quad (10)$$

It is of interest to examine several of these expressions.

The direct current that flows in the step at zero voltage i.e., the zero-voltage current is given by

$$j_{dc}(\omega_0=0)/j_0 = J_0(P_1) J_0(P_2) \sin\varphi_0, \quad (11)$$

where $P_1 = 2ev_1/\hbar\omega_1$ and $P_2 = 2ev_2/\hbar\omega_2$. Equation (11) shows the explicit dependence of the zero-voltage current on the power level of both applied rf voltages. Although the derivation assumed that the dc voltage was specified, Eq. (11) also demonstrates that, on a constant-voltage step, control of the current from an external source is tantamount to fixing a phase factor. Here, for the zero-voltage current, the phase φ_0 is determined whenever the current is constrained to some value by an external circuit. As is shown explicitly below in another case, other phase factors, combinations of φ_0 , θ_1 , and θ_2 , play the same role on other constant-voltage steps.

It is also possible to calculate the current flowing at any specific frequency with the junction biased on the zero-voltage step. In particular, the current at the difference frequency is

$$j_{\Delta\omega}(\omega_0=0)/j_0 = -J_1(P_1) J_1(P_2) 2 \sin\varphi_0 \cos[(\omega_1 - \omega_2)t + (\theta_1 - \theta_2)]. \quad (12)$$

Here, too, the amplitude of the current depends on both rf voltage amplitudes and the phase factor φ_0 .

It is also of interest to examine the current that flows in some of the additional steps that result from the mixing action. For explicitness, assume $\omega_1 > \omega_2$, then consider the step at $\omega_0 = \Delta\omega$, i.e., $\omega_0 = \omega_1 - \omega_2$. The direct current on that step is

$$j_{dc}(\omega_0 = \Delta\omega)/j_0 = -J_1(P_1) J_1(P_2) \sin[\varphi_0 - (\theta_1 - \theta_2)], \quad (13)$$

and the current at the difference frequency is

$$j_{\Delta\omega}(\omega_0 = \Delta\omega)/j_0 = \{ J_0^2(P_1) J_0^2(P_2) + J_2^2(P_1) J_2^2(P_2) - 2J_0(P_1) J_0(P_2) J_2(P_1) J_2(P_2) \cos 2[\varphi_0 - (\theta_1 - \theta_2)] \}^{1/2} \times \cos[(\omega_1 - \omega_2)t + (\theta_1 - \theta_2) - \Phi_{\Delta\omega}], \quad (14)$$

where

$$\Phi_{\Delta\omega} = \tan^{-1} \left\{ \frac{J_0(P_1) J_0(P_2) - J_2(P_1) J_2(P_2)}{J_0(P_1) J_0(P_2) + J_2(P_1) J_2(P_2)} \times \cot[\varphi_0 - (\theta_1 - \theta_2)] \right\}. \quad (15)$$

In both Eqs. (13) and (14) the phase factor $\varphi_0 - (\theta_1 - \theta_2)$ appears and plays the same role that φ_0 alone did in Eqs. (11) and (12). The appearance of $\theta_1 - \theta_2$ reflects the fact that the dc voltage, i.e., the "Josephson frequency," ω_0 , is equal to $\omega_1 - \omega_2$ on the step under study. A similar combination appears appropriate to the value of ω_0 for each step.

¹⁶ W. G. Bickley, *Bessel Functions and Formulae* (Cambridge University Press, England, 1957), formulas 94a and 94b.

¹⁷ S. Shapiro, *Phys. Rev. Letters* **11**, 80 (1963); S. Shapiro, A. R. Janus, and S. Holly, *Rev. Mod. Phys.* **36**, 223 (1964).

From Eqs. (11) and (13) it is apparent that the maximum dc current that can flow in a constant-voltage step in the presence of two rf voltages is determined by the product of two Bessel functions. To facilitate comparison with experimental results in Sec. IV, Table I displays for several steps the Bessel-function products obtained from expressions similar to Eqs. (11) and (13).

Although the equations derived so far are generally valid, no attempt has been made to introduce a "linewidth," or voltage spread, for the constant-voltage steps. Such a voltage spread or, what is the same thing, a line shape for the Josephson frequency, occurs in any real experimental situation because of thermal noise, current fluctuations, and phase noise. However, rather than attempting to introduce any such linewidth parameter in the analysis presented up to now, we prefer to take an entirely different approach in discussing one case to which many of our experiments apply.

Many data were taken with both applied frequencies nearly equal and with the amplitude of one much larger than the amplitude of the other. In this case we simply note that the two signals add to produce a beat signal which is equivalent to a single signal amplitude modulated to a small extent at the difference frequency. Using this equivalence we shall show in Sec. IV B that the results of our experiments with two signals of nearly equal frequency are readily explained by a model which treats the Josephson junction as a high-frequency video detector.^{8,9,17}

III. EXPERIMENTAL DETAILS

A. Preparation and Characterization of Point-Contact Junctions

Adjustable point-contact Josephson junctions formed from superconducting niobium (Nb) were used almost exclusively. The junctions were formed by pressing together the ends of two pieces of Nb wire, one of which was flattened and the other pointed by a chemical etch. Thirty-mil-diam wire proved to be a convenient size.

The junction was formed about midway across the narrow dimension of either *M*-band (0.148 in. \times 0.074 in.) or *K*-band (0.42 in. \times 0.17 in.) waveguide. The Nb wires were introduced through small, insulated holes in opposite waveguide walls. Leads for providing bias and for measuring the voltage-current characteristic of the junction were soldered outside the waveguide to pointed brass screws which in turn were pressed hard against the niobium wires for electrical contact. The mechanism for adjusting the junction *V-I* curve made use of a differential screw and was similar to that described elsewhere.^{9,18} The junction was immersed directly in liquid helium and was formed and adjusted *in situ*.

The range of *V-I* characteristics obtainable for adjustable point-contact Josephson junctions has been

¹⁸ A. Contaldo, Rev. Sci. Instr. **38**, 1543 (1967).

described in some detail elsewhere.⁹ It suffices to point out here that care was taken to use in our mixer experiments, junctions whose Josephson-effect behavior was similar to thin-film Josephson-tunnel junctions. Thus, for the most part, junctions were selected for study that had rather low values of zero-voltage current, that were free of hysteresis regions in their *V-I* curves, and that showed constant-voltage steps, in the presence of a single applied rf voltage, mostly at those voltages expected for simple Josephson-tunnel junctions, i.e., at $\omega_0 = n\omega$.

Figure 1 shows a series of *V-I* curves for a Nb-Nb junction exposed to rf at only one frequency; and Fig. 2 is a comparison of the data of Fig. 1, for several constant-voltage steps, with the Bessel-function dependence on rf voltage expected from simple theory that pertains to weak-coupled, or tunnel, junctions. The scales for all the data of Fig. 2 were set by fitting to the two circled data points on the curve for the $n=1$ step. The agreement between theory and experiment is at least as good as that reported earlier for a thin-film tunnel junction¹⁷ except near zero rf voltage on the $n=0$ step. The large excess current for the $n=0$ step at small values of rf voltage is attributed to current flowing through microscopic metallic bridges in parallel with the Josephson tunneling current.¹⁹ This excess current is quenched monotonically as the rf voltage and current are increased. The agreement between theory and experiment, the clarity of the step structure of the *V-I* curves of Fig. 1, and the absence of any but expected structure in the *V-I* curves all demonstrate our success in obtaining junctions with the desired tunnellike behavior for the mixer experiments.

TABLE I. Bessel functions governing amplitudes of constant-voltage steps when two rf voltages at angular frequencies ω_1 and ω_2 are applied.

Josephson frequency at constant-voltage step (value of $2eV_{dc}/\hbar$ sec ⁻¹)	Bessel-function product governing dc current amplitude on constant-voltage step ^a
0	$J_0(P_1) J_0(P_2)$
$\Delta\omega \equiv \omega_1 - \omega_2$	$J_1(P_1) J_1(P_2)$
$\omega_2 - \Delta\omega$	$J_1(P_1) J_2(P_2)$
ω_2	$J_0(P_1) J_1(P_2)$
ω_1	$J_1(P_1) J_0(P_2)$
$2\omega_2$	$J_0(P_1) J_2(P_2)$
$\omega_1 + \omega_2$	$J_1(P_1) J_1(P_2)$

^a The Bessel-function arguments P_1 and P_2 are defined respectively as $2ev_1/\hbar\omega_1$ and $2ev_2/\hbar\omega_2$, where v_1 and v_2 are the amplitudes of the voltages at frequencies ω_1 and ω_2 .

¹⁹ P. W. Anderson and A. H. Dayem, Phys. Rev. Letters **13**, 195 (1964); A. H. Dayem and J. J. Wiegand, Phys. Rev. **155**, 419 (1967).

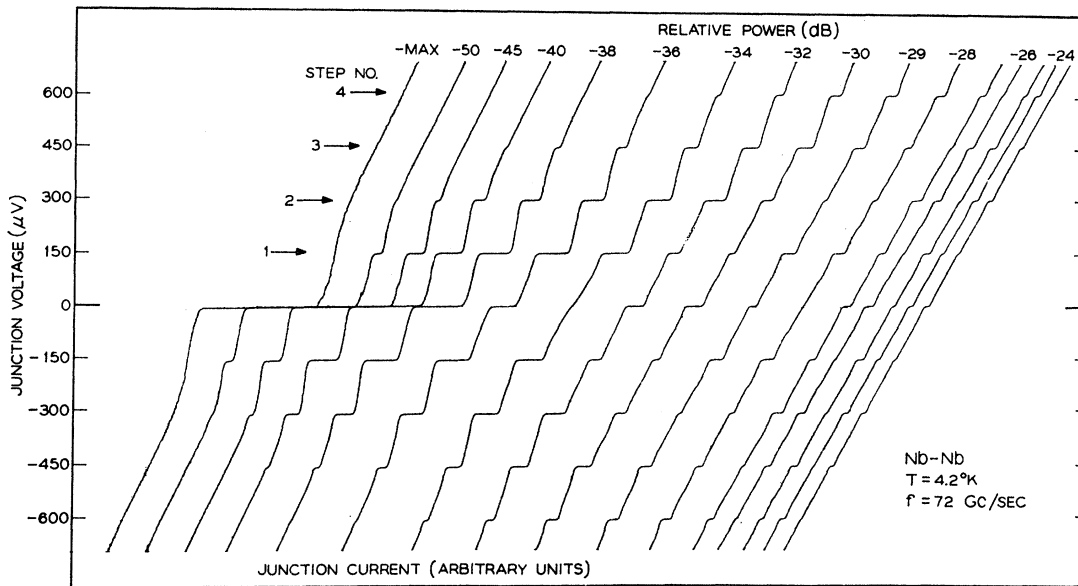


FIG. 1. Voltage-current curves for a Nb-Nb point-contact Josephson junction exposed to a 72-Gc/sec signal at various power levels.

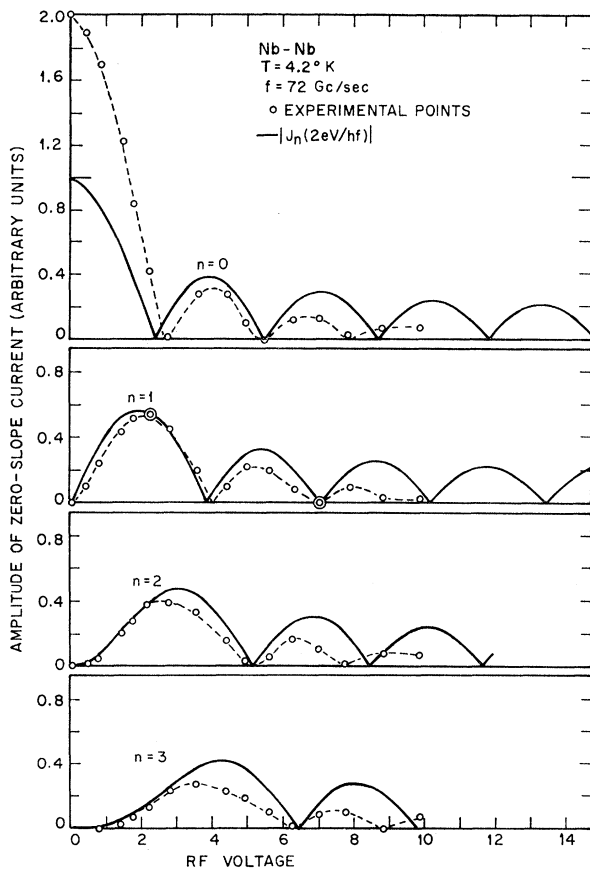


FIG. 2. Data from Fig. 1 plotted to display how the current in several constant-voltage steps varies as the applied rf voltage is varied. The data points from the n th step are compared with the amplitude of the n th-order Bessel function which is the behavior expected for an ideal tunnel junction. The data were fitted to the theoretical curves at the two points denoted by double circles. The rf voltage across the junction is expressed in units of $hf/2e$ or 149 μ V per division.

Some junctions were tested that had more or less prominent subharmonic structure in their V - I curves in the presence of rf. Such structure, which occurs at voltages given by $m\omega_0 = n\omega$, is characteristic of metallic bridges¹⁹ between the superconductors forming the junction. A mixed-frequency signal associated with the subharmonic steps was observed similar to that described later associated with the main steps. However, no detailed study of such junctions was undertaken and attention is confined in the balance of this paper to the behavior of junctions similar to that of Figs. 1 and 2.

B. Equipment and Procedures

A schematic block diagram, applicable to all the mixing experiments, is shown in Fig. 3. The signals from each of two separate rf sources, labeled klystron A and klystron B, passed along a waveguide containing a ferrite isolator, a wavemeter and a precision attenuator before being combined in a waveguide "tee." Thus each source was isolated from the other as well as from junction reflections and both the frequency and amplitude of each source could be separately measured and adjusted. The combined rf signals passed into the helium Dewar via a section of appropriately sized waveguide and fell onto the junction mounted across the waveguide near its termination. The waveguide was left open at its end. The mixed frequency, or intermediate frequency (i.f.), was on the order of 1 Mc/sec and was brought out via a coaxial line connected directly across the voltage terminals of the junction. The i.f. was amplified in a Tektronix type 1A7 rf amplifier. The output of the amplifier was in turn rectified and, when desired, switched to the Y terminals of a Moseley 7000-A X-Y recorder where it was plotted as the i.f. amplitude. The junction bias

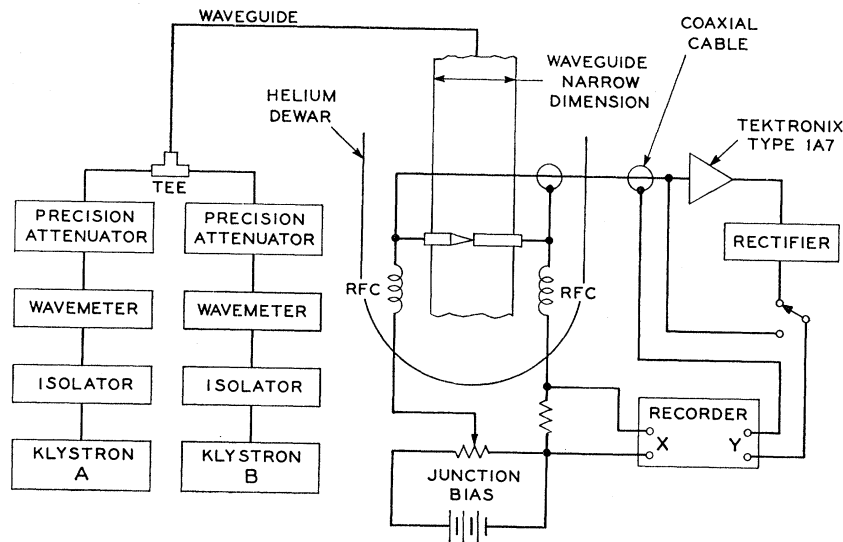


FIG. 3. Schematic block diagram of the mixer experiments. The point-contact Josephson junction is mounted across the waveguide in the helium Dewar.

circuitry was isolated from the i.f. signal by rf chokes, labelled RFC in Fig. 3. The voltage across a resistor in series with the junction was fed to the X terminals of the recorder and plotted as the junction current. The dc voltage across the junction was fed through a switch to the Y terminals of the recorder. Thus both the junction voltage and the i.f. amplitude were plotted alternately on the X-Y recorder. Although not shown in Fig. 3, ac junction bias and an X-Y oscilloscope, Tektronix type 502A, were also used occasionally for displaying junction V - I characteristics.

For the experiments at 23 Gc/sec, two K -band klystrons were used. For the experiments at 72 Gc/sec, one source was an M -band klystron Raytheon type QKK1150; the second source, provided by Copeland and Spiwak, consisted of a bulk gallium arsenide diode oscillating in the LSA (limited space-charge accumulation) mode.²⁰ For some experiments the LSA oscillator operated at 72 Gc/sec while the M -band klystron was tuned to about 64 Gc/sec. In other experiments the LSA oscillator was used at 72 Gc/sec while a K -band klystron was used as the second source at 24 Gc/sec, i.e., at one-third the LSA oscillator frequency.

In general, our experimental procedure was as follows: With the source frequencies set, the junction V - I curve was adjusted until it was considered acceptable according to the criteria enumerated earlier. Then one source was set at a power level sufficient to produce several constant-voltage steps in the V - I curve. Frequently some particularly well-defined power level was chosen, e.g., such as to produce the first zero in the $n=0$ step, or maximize the $n=2$ step, etc. (see Fig. 2). Data would then be taken for a large number of reasonably close together power levels from the second source. At each power setting a recorder tracing

was made of junction voltage versus junction current and also of i.f. amplitude versus junction current. The junction current was swept by a motor-driven single-wire potentiometer.

IV. EXPERIMENTAL RESULTS

A. Inputs at 72 and 64 Gc/sec

As shown in Sec. II, the clearest distinction between the Josephson mixing mechanism and classical nonlinear mixing is provided by the prediction, for the former, of constant-voltage steps in the V - I curve separated by the voltage appropriate to the difference frequency. Such steps were observed, as shown in Fig. 4, when a signal at 72 Gc/sec from the LSA oscillator was mixed in a Nb-Nb junction against a signal at 64 Gc/sec from the M -band klystron.

The LSA oscillator was first set at a fixed power level sufficient to generate one or more constant-voltage steps (e.g., Fig. 4, second curve from the left) at 150- μ V intervals corresponding to the LSA frequency of 72 Gc/sec. Then a series of curves was taken with the klystron source gradually increased in power level. As klystron power was increased, steps at 132- μ V intervals were seen (e.g., Fig. 4 curve at -26 dB) as expected for the 64-Gc/sec source. Additional steps, arising from the difference frequency of 8 Gc/sec were also seen (e.g., Fig. 4, curve at -26 dB), separated from the steps noted above by about 16 μ V.

The data of Fig. 4 were taken with a moderate level of LSA power. Additional sequences were taken with both lesser and greater LSA power. It is important to note that *all* such data for any one junction are interrelated in such a way that calibration of the power scales and of the relative amplitudes at any two data points fixes the power variation of the step current in *all* steps.

²⁰ J. A. Copeland, Proc. IEEE 54, 1479 (1966); IEEE Spectrum 4, No. 5, 71 (1967).

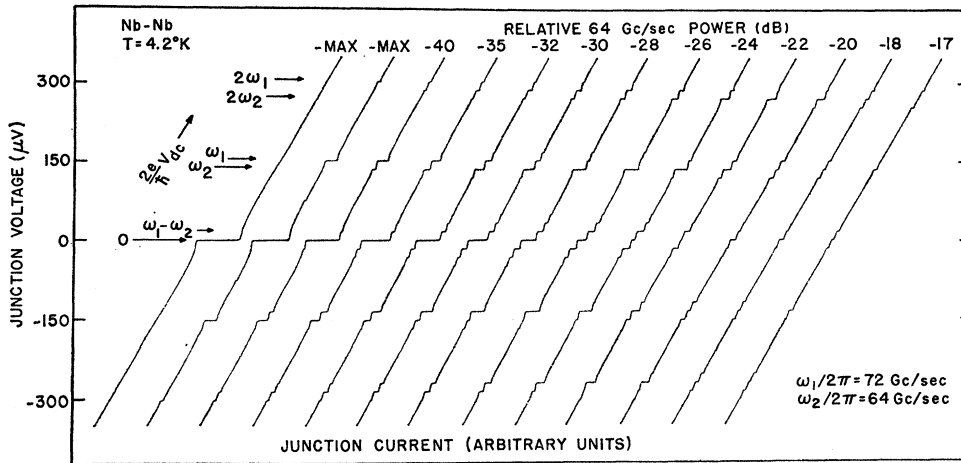


FIG. 4. The curve on the left is a $V-I$ curve in the absence of microwave power. The remaining curves are a series of $V-I$ curves with variable power from a source at 64 Gc/sec mixing with fixed power from a source at 72 Gc/sec. The constant-voltage steps are labelled with the Josephson angular frequency corresponding to the voltage at the step. The 72-Gc/sec power produces the steps at ω_1 and $2\omega_1$ while the 64-Gc/sec power produces the steps at ω_2 and $2\omega_2$. Mixing action produces the remaining steps. Note especially the additional steps at the difference frequency $(\omega_1 - \omega_2)$ and at multiples of the difference frequency.

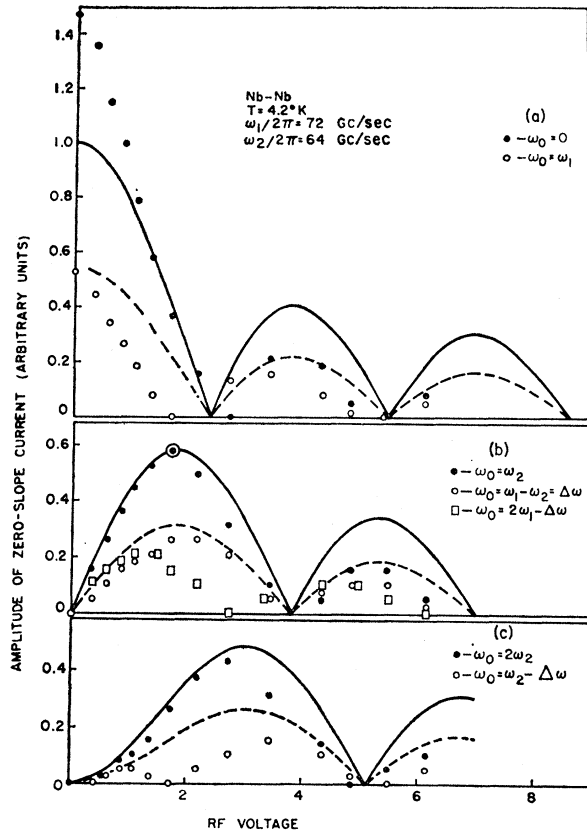


FIG. 5. Data of Fig. 4 plotted to compare the current in several constant-voltage steps with the Bessel-function dependence expected for a tunnel junction. The solid data points are to be compared with the solid theoretical curves, and the open data points are to be compared with the dashed theoretical curves. The expressions for all theoretical curves are tabulated in Table I. Data and theory were fit at only one point, viz., at the first maximum of the data for $\omega_0 = \omega_2$. The rf voltage across the junction is expressed in units of $hf/2e$ or $132 \mu\text{V}$ per division.

In Fig. 5 we present one way of demonstrating the interrelationship of the data and also of comparing it with the variations predicted from the analysis in Sec. II. In this figure we have plotted the amplitudes of the constant-voltage steps measured on the $V-I$ curves in Fig. 4. The data points in Fig. 5 are grouped in parts (a), (b), and (c) according to the $J_0(P_2)$, $J_1(P_2)$, and $J_2(P_2)$ Bessel-function dependence on rf voltage predicted by the Josephson equations and tabulated in Table I. The solid theoretical curve in part (b) was fitted to the data point at the peak of the first maximum. Fitting to this one data point determines the Bessel-function argument P_2 and the ordinate scale used to plot *all* of the theoretical curves. The Bessel-function argument P_1 was determined by noting the LSA source level required to maximize the step at $\omega_0 = \omega_1$ in the absence of the klystron signal. The agreement between predicted and observed behavior is satisfactory for most of the steps. The large excess current for the $\omega_0 = 0$ step shown in Fig. 5(a) at small values of P_2 has the same origin as it did in Fig. 2; i.e., it arises from current flowing through microscopic metallic bridges in parallel with the Josephson-tunneling current. This excess current is quenched monotonically as P_2 increases. Since a current source was used to obtain the $V-I$ traces in Fig. 4, the voltage is a single-valued function of current. Hence, use of a current source prohibits observation of any multiple-valued portions of the $V-I$ curve and contributes to the remaining discrepancies in Fig. 5. For example, in Fig. 5(c), the data points for the $\omega_0 = \omega_2 - \Delta\omega$ step go to zero at a smaller value of P_2 than expected. At this value of P_2 the step at $\omega_0 = \omega_2$ has reached its maximum amplitude where it overlaps and tends to obscure the step at $\omega_0 = \omega_2 - \Delta\omega$.

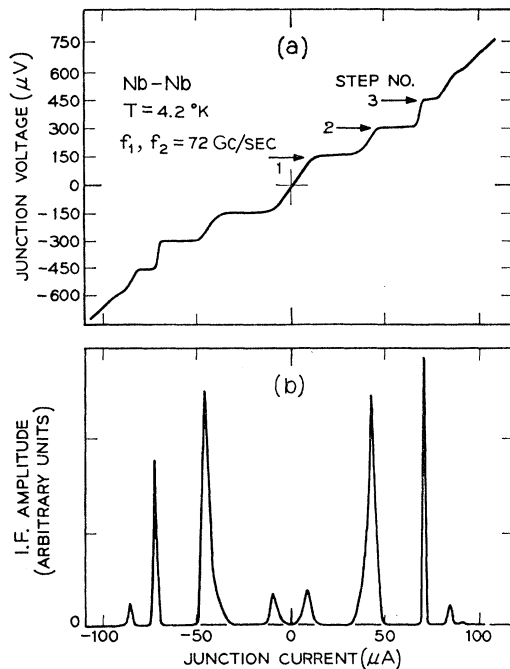


FIG. 6. Junction voltage (a) and i.f. amplitude (b) plotted versus junction current for two applied signals at 72 Gc/sec. Power level of one source is set such that the zero-voltage current is approximately at its first zero. Some other constant-voltage steps are labelled. Ratio of powers is about six to one. The i.f. is at about 1 Mc/sec.

B. Two Inputs at about 72 Gc/sec

With the experimental setup and procedure detailed in Sec. III, many data were taken on mixing of two signals at 72 Gc/sec differing only by about 1 Mc/sec. The arrangement for detecting and plotting the i.f. amplitude passed a rather broad band of frequencies and so did not discriminate between the dominant difference frequency term or its first few harmonics, all of which are present to greater or lesser degree as is clear from the discussion and equations of Sec. II. However, the effect of i.f. harmonics is expected to be minimal for several reasons. The procedure followed was to tune the frequency of the klystron source towards that of the LSA source until an i.f. signal was observed on a high-frequency oscilloscope (Tektronix type 547) at the output of the rf amplifier. Thus the i.f. was always toward the high end of the amplifier pass-band, reducing the effect of harmonics, and the output waveform directly observed was never very much different from a sine wave. Furthermore, some runs were made with the Tektronix 1A7 amplifier replaced by a broadband amplifier with a pass-band from 0.8 to 150 Mc/sec. The results obtained using this much higher i.f. were similar to those with an i.f. of only about a megacycle per second.

Figure 6 shows representative data. The i.f. amplitude and junction voltage are plotted, in separate curves, versus the junction current. The LSA source

was set at a power level about six times that of the klystron and sufficient to produce constant-voltage steps as labelled in the $V-I$ curve, Fig. 6(a). The power was such as to achieve approximately the first zero in the zero-voltage current (see Fig. 2, $n=0$). The i.f. amplitude obtained under these conditions is shown in Fig. 6(b). The i.f. amplitude exhibits peaks at values of junction current such that the junction is biased in between constant-voltage steps. When the junction is biased to the beginning or end of a step, the i.f. amplitude falls very rapidly towards zero. Examination of many pairs of curves taken for many different combinations of power level yielded the same result as the data of Fig. 6; namely, the i.f. amplitude always exhibits peaks at bias currents in between steps and always falls rapidly towards zero at bias currents on steps.

Although puzzling at first sight, this behavior is readily accounted for by the considerations of Sec. II. There it was pointed out that two applied signals that are nearly equal in frequency beat together and are equivalent, with respect to their effect on the $V-I$ curve and on the frequency spectrum of the Josephson current, to one applied signal whose amplitude is modulated to a small extent at some slowly varying rate. Thus the junction responds to a signal with a quasistatic power level and easily follows the slow variations in power level; i.e., the junction demodulates the effective carrier. It is shown elsewhere⁹ that the response time of a point-contact Josephson junction detector is less than 10 nsec. Thus the demodulation model should hold for two signals that differ in frequency by at least as much as 100 Mc/sec and therefore is applicable to our experiments.

In the demodulation, or video detector, model variations at the i.f. in the applied power result in variations at the i.f. in the maximum current that can flow in the constant-voltage steps. These current variations are converted into output-voltage variations exactly as in the earlier high-frequency video-detection experiments.^{8,9} Figure 7 indicates how the voltage output is produced for the particularly simple case where the

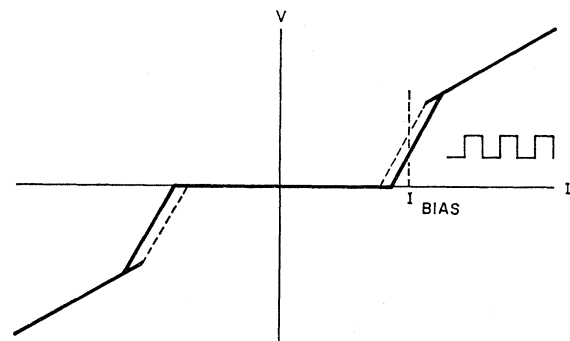


FIG. 7. Schematic $V-I$ curve showing how an applied rf signal causes a change in zero-voltage current which is converted to a voltage output by constant-current external bias. Dashed curve is for rf on, solid curve for rf off.

bias current is slightly greater than the zero-voltage current and where there is only one applied rf signal which is being turned on and off. The V - I curve in the absence of applied power is sketched as the solid curve. Constant-current bias is used, as indicated, to some point of high slope. In the presence of applied power, the V - I curve is modified to that indicated in the sketch by the dashed lines. Since the junction current cannot change because of the constant-current external bias circuitry, the voltage across the junction shifts. As the power is turned on and off, the junction voltage varies approximately as a square wave as indicated in the figure. The amplitude of the voltage signal will depend not only on the change in zero-voltage current but also on the slope in the V - I curve at the bias point. Thus the conversion gain is proportional to the differential resistance of the junction at the bias point.

In contrast, classical mixer theory predicts an output signal proportional to the curvature of the V - I curve, i.e., d^2V/dI^2 . It is a simple matter to distinguish between the classical prediction d^2V/dI^2 and the Josephson modulation mechanism which includes the gain factor dV/dI .

In the Josephson junction mixer, the effective amplitude variation of the input signal produces an output voltage which varies at the same rate. For a small enough effective depth of modulation, the conversion gain during the modulation period is constant since the V - I curve at the bias current is not changed in shape. This accounts for the peaking in the i.f. voltage in between constant-voltage steps since there the junction differential resistance also peaks. On the other hand, the curvature of the V - I curve goes to zero in between steps. Our observations clearly show the Josephson mixing mechanism to be operating as opposed to classical mixing. Since the differential resistance on a step is essentially zero, the conversion gain on a step and, consequently, the i.f. amplitude are also zero as observed.

At the beginning and end of a step, the V - I curve is drastically modified during a modulation cycle and, correspondingly, the conversion gain is not constant during a cycle when the junction is biased at such points. Rather some average value comes into play, a value determined by the amount of time during a modulation cycle that the slope of the V - I curve at the bias current differs from zero. Thus the i.f. amplitude should fall rapidly toward zero for bias currents at the beginning or end of a constant-voltage step as is observed.

Although this Josephson video-detection mechanism accounts well qualitatively for the mixer results, it is not possible to express it in any simple quantitative form. This is because the modification in the V - I curve at bias currents just beyond the $n=1$ step, e.g., is not only produced by changes with applied power of the current in that step but also is produced by changes in the zero-voltage current. Similar but even more complicated considerations apply at other bias points.

Nevertheless, it is possible to see from data such as in Fig. 6 how the variations of Josephson current in a step affect the heights of i.f. amplitude peaks. For example, the data of Fig. 6 were selected from a series of data and correspond to a region of applied power where the zero-voltage current is practically zero over a small range of power. On the other hand, the $n=1$ and $n=2$ steps show appreciable shifts for small changes in applied power. Correspondingly, the i.f. amplitude near zero current is very much smaller than the next two peaks which are associated largely with changes in the $n=1$ and $n=2$ steps. The relative amplitudes of the peaks are, of course, also affected by the different conversion gain factors dV/dI applicable in each case.

The i.f. amplitude data of Fig. 6 show one more characteristic worthy of comment; they are almost but not quite symmetric in current. Josephson's equations, of course, are symmetric. The experimental asymmetry results from one or more of a number of factors; asymmetry of the V - I curve, asymmetry in step current resulting from small amounts of flux trapped in the junction, and, most important, drift of the rf sources during the several minutes required to record the data, so that the power levels are not precisely the same for all parts of the data curves. Since the junction mixer is so sensitive to small power changes and to the detailed shape of the V - I curve, asymmetry in the data from the above sources was virtually impossible to avoid. Gross changes in the V - I curve during data runs, from such causes as electrical transients or mechanical shock, were readily noticeable and taken into account.

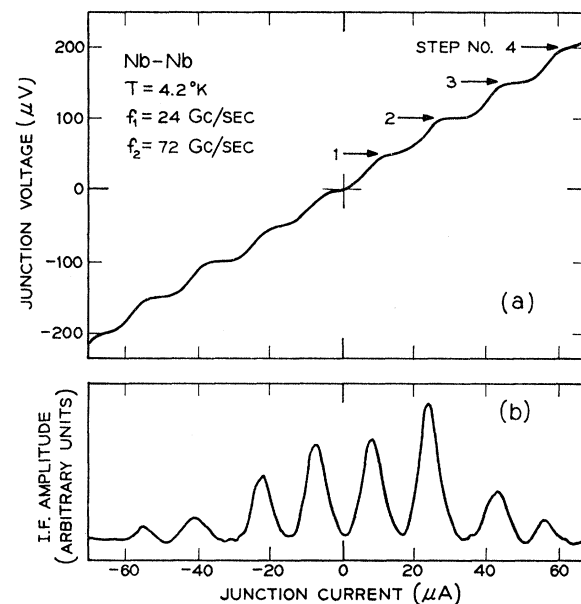


FIG. 8. Junction voltage (a) and i.f. amplitude (b) plotted versus junction current when two signals are applied—one at 72 and one at 24 Gc/sec whose third harmonic is involved in mixing. The 24-Gc/sec power level is such as to yield a maximum, approximately, in constant-voltage step No. 2. Ratio of powers is about 5:1. The i.f. is at about 1 Mc/sec.

C. Two Inputs at about 23 Gc/sec

Experiments similar in all respects to those employing two 72-Gc/sec sources were also carried out with two 23-Gc/sec sources. The remarks in the last section regarding experimental procedure, V - I curves, and i.f. amplitude curves also apply here. The results were similar to those already presented and discussed and so no further discussion of the 23-Gc/sec results is given.

D. Inputs at 72 and 24 Gc/sec

A signal at 72 Gc/sec will propagate in K -band waveguide. A junction mounted across K -band waveguide was exposed to a signal at 72 Gc/sec by using a series of adapters to introduce the LSA source output into the experimental K -band rig. The 72-Gc/sec power level at the junction was about one-fifth that of a 24-Gc/sec signal also brought onto the junction.

Figure 8 shows representative data. Figure 8(a) is a plot of a junction V - I curve showing the constant-voltage steps, separated by about $50 \mu\text{V}$, corresponding to the 24-Gc/sec signal. The power level was set to maximize, approximately, the current in step No. 2. Figure 8(b) gives the corresponding curve of i.f. amplitude versus junction current. The third harmonic of the 24-Gc/sec signal differed from the 72-Gc/sec signal by the i.f. of about 1 Mc/sec.

Using the general relation for the Josephson current in a junction exposed to two rf signals, Eq. (9), with the substitution $\omega_1 = 3\omega_2 + \Delta\omega$ applicable to this case, expressions similar to Eqs. (11)–(15) can be derived. Such expressions demonstrate that the i.f. term arises from the mixing of the 72-Gc/sec signal ω_1 against the third harmonic of the 24-Gc/sec signal ω_2 .

The data of Fig. 8 are similar to the data of Fig. 6 for two 72-Gc/sec inputs and are understood on the same basis. For example, with the power level set so that step No. 2 is near its first maximum, the current in that step is relatively insensitive to small power changes and so the peak in i.f. amplitude associated largely with step 2 is weak. That the peak is as high as it is follows in part from the higher value of conversion

gain dV/dI associated with that peak in comparison to others.

Finally, we note that it should be possible to use a Josephson junction as its own local oscillator.¹⁵ For an input signal at ω_1 , and with the junction biased such that $\omega_0 = \omega_1 + \Delta\omega$, an i.f. signal at $\Delta\omega$ should be produced. Such behavior was searched for, but not found presumably because we did not take sufficient care to provide proper constant-voltage bias. Stray pick-up in the bias circuit of as little as 10^{-8} V was sufficient to shift the difference frequency out of the pass-band of our i.f. amplifier.

V. SUMMARY

We have demonstrated through experiments at 23 and at 72 Gc/sec that two microwave or millimeter-wave signals mix in a point-contact Josephson junction. The mixing action manifests itself by changes in the dc V - I characteristic of the junction and by generation of i.f. signals. Both of these manifestations have been observed in our experiments. An analysis based on Josephson's phenomenological equations has shown that Josephson mixing, in contrast to classical nonlinear mixing, gives rise to additional constant-voltage steps in the junction V - I curve which we have observed. In addition, two signals of nearly equal frequency yield an i.f. signal that varies, among other factors, with the differential resistance dV/dI of the junction. This variation has also been observed in our experiments and is in sharp contrast to the classical result that the i.f. amplitude varies as the curvature d^2V/dI^2 of the junction characteristic.

Thus we have provided an experimental demonstration of the existence of the Josephson mixing mechanism, derived relevant equations, and demonstrated its dependence on frequency, power level, and junction V - I curve.

ACKNOWLEDGMENTS

We are deeply indebted to G. Adams for taking the bulk of the experimental data. We are extremely grateful to J. A. Copeland and R. R. Spiwak for providing the 72-Gc/sec LSA oscillator used in the experiments.